

Letter to the Editor on the ACP manuscript “An estimation of the $^{18}\text{O}/^{16}\text{O}$ ratio of UT/LMS ozone based on artefact CO in air sampled during CARIBIC flights” by S. Gromov and C. A. M. Brenninkmeijer

S. Gromov, on behalf of all authors
sergey.gromov@mpic.de

Dear Dr. Kaiser,

With this letter we would like to summarise the changes and updates to the manuscript we have introduced preparing the revised version of our paper. We have considered all comments and accepted all of the suggestions proposed by the Referees, except a few instances that either were unclear to us or arouse from what we believe was a misunderstanding by the Referee #1 (please see the Author Comment submitted earlier for detailed answers).

The structure of the manuscript underwent minor modifications. We introduced subsections in Sect. 2 and relocated the information to amend the content flow, *i.e.* the on-line and WAS instrumentation setup, followed by the description of the results. Some discussion was moved from Sect. 2 to Sect. 3.

The content of the manuscript was amended substantially in Introduction (this section is almost rewritten), whilst minor improvements were introduced in Sects. 2.3, 3, 3.2. Two more references were added (Savarino and Morin, Stevens *et al.*). Furthermore, Fig. 1 was extended and Fig. 2 was corrected due to the error in our plotting software. We have added the Supplementary Material to the manuscript which includes four more figures requested by the Referees. Please see all changes between the manuscripts submitted to ACPD and ACP marked up in the following pages. Please note that we would like to leave the decision on some technical issues (*e.g.*, use of the double superscript plus subscript notation) at your discretion.

Finally, our final Author Comment ([AC C7938](#), pp. C7938–C7956) enumerates all referee comments and suggestions and the measures we have taken to address them. We appreciate very much the time you spent for editing this paper.

With best regards,

Sergey Gromov

Deleted: LS

An estimation of the $^{18}\text{O}/^{16}\text{O}$ ratio of UT/LMS ozone based on artefact CO in air sampled during CARIBIC flights

S. Gromov¹, C. A. M. Brenninkmeijer¹
¹ Max Planck Institute for Chemistry, Mainz, Germany
Correspondence to: S. Gromov (sergey.gromov@mpic.de)

1 Abstract

2 | An issue of O_3 -driven artefact production of CO in the UT/LMS air analysed in the
3 | CARIBIC-1 project is being discussed. By confronting the CO mixing/isotope ratios obtained
4 | from different analytical instrumentation, we (i) Reject natural/artificial sampling and mixing
5 | effects as possible culprits of the problem, (ii) Ascertain the photochemical nature and quantify
6 | the strength of the effect in a general contamination kinetic framework, and (iii) Demonstrate
7 | the successful application of the isotope mass-balance calculations for inferring the isotope
8 | signature of the contamination source. The $^{18}\text{O}/^{16}\text{O}$ ratios of the latter unambiguously indicate
9 | the oxygen being inherited from O_3 . The $^{13}\text{C}/^{12}\text{C}$ ratios hint at reactions of trace amounts of
10 | organics with ample stratospheric O_3 that could have yielded the artificial CO. While the exact
11 | contamination mechanism is not known, it is clear that the issue pertains only to the earlier
12 | (first) phase of the CARIBIC project. Finally, estimated UT/LMS ozone $^{18}\text{O}/^{16}\text{O}$ ratios are
13 | lower than those observed in the LMS within the same temperature range, suggesting that
14 | higher pressures (240–270 hPa) imply lower isotope fractionation controlling the local $\delta^{18}\text{O}(\text{O}_3)$
15 | value.

Deleted: ozone

Deleted: 1

Deleted: 2

Deleted: , (3

Deleted: ozone

Deleted: inhibit

16 1 Introduction

17 | [1] Successful determination of the atmospheric carbon monoxide (CO) content based on the
18 | collection of air samples depends on the preservation of the mixing ratio of CO inside the

19 receptacle, from the point of sampling to the moment of physiochemical analysis in a
 20 laboratory. A well known example in our field of research is the filling of pairs of glass flasks at
 21 South Pole Station for analysis at NOAA in Boulder, Colorado, USA (Novelli *et al.*, 1998).
 22 There, the duplicate air sampling allowed for a degree of quality control which in view of the
 23 long transit times, especially during polar winter, was a perhaps not perfect, but certainly a
 24 practical measure. Here we deal with a different case: Using aircraft-based collection of very
 25 large air samples rendered duplicate sampling unpractical, yet analyses could be performed
 26 soon after the sampling had taken place because of the proximity of the aircraft's landing
 27 location to the laboratory involved. A presumption of the analytical integrity of the process was
 28 that the growth of CO in receptacles is gradual and takes its time. Reminding Thomas Henry
 29 Huxley's statement, "The great tragedy of Science – the slaying of a beautiful hypothesis by an
 30 ugly fact", it turned out, however, that for air we collected in stainless steel tanks in the upper
 31 troposphere/lowermost stratosphere (UT/LMS) higher CO values were measured in the
 32 laboratory than measured *in situ* during the collection of these air samples. Moreover,
 33 measurement of the stable oxygen isotopic composition of CO from these tanks revealed
 34 additional isotopic enrichments in ¹⁸O of 10‰ or more. It was soon realised that this
 35 phenomenon was due to the formation of CO in these tanks and/or possibly in the sampling
 36 system and inlet tubing used, by reactions involving ozone (Brenninkmeijer *et al.*, 1999).
 37 [2] Unexpectedly high ¹⁸O/¹⁶O ratios in stratospheric ozone (O₃) were discovered by Konrad
 38 Mauersberger using a balloon-borne mass spectrometer (Mauersberger, 1981), which has
 39 triggered a series of theoretical and experimental studies on atmospheric O₃ heavy isotope
 40 enrichments (see, e.g., Schinke *et al.* (2006) for a review). In view of the advances in theoretical
 41 and laboratory studies on the isotopic composition of O₃ atmospheric measurements are
 42 welcome, they do however form a challenge. In the stratosphere O₃ is abundant, but the
 43 remoteness of the sampling domain is a problem. In the troposphere, low O₃ concentrations are
 44 the main obstacle, as indicated by few experiments performed to date (Krankowsky *et al.*, 1995;
 45 Johnston and Thiemens, 1997; Vicars and Savarino, 2014). Nevertheless, recent analytical
 46 improvements, namely the use of an indirect method of reacting atmospheric O₃ with a
 47 substrate that can be analysed for the isotopic composition of the O₃-derived oxygen
 48 (Vicars *et al.*, 2012), has greatly improved our ability to obtain information on the O₃ isotopic
 49 composition.
 50 [3] Although the increase of CO concentrations in air stored in vessels is a well recognised
 51 problem, to our knowledge a specific O₃-related process has not been reported yet. Here we

- Deleted: famous
- Deleted: the much later
- Deleted: ,,
- Deleted: Such was not the case
- Deleted: study presented here: For air collected in stainless steel tanks in the upper troposphere/lowermost stratosphere (UT/LMS) we observed higher CO values than measured concomitantly
- Deleted: -*situ*. Moreover, measurement of the stable oxygen isotopic composition of CO from these tanks indicated additional isotopic enrichments in ¹⁸O of 10‰
- Deleted: greater. It was soon realised that this phenomenon was due to the formation of CO in these tanks and/or in the sampling system and inlet tubing used, by reactions involving ozone (Brenninkmeijer *et al.*, 1999).¶ Unexpectedly high ¹⁸O ... [1]
- Deleted: causes
- Deleted: the atypical ... [2]
- Deleted: studies of
- Deleted: nature
- Deleted: However, ... [3]
- Deleted: ozone is ge ... [4]
- Deleted: its concent ... [5]
- Deleted: ,,
- Deleted: ,
- Deleted: ,
- Deleted: The
- Deleted: ozone
- Deleted: -
- Deleted: helps a goc ... [6]
- Deleted: ,,
- Deleted:).
- Deleted: The air san ... [7]
- Deleted: ozone

52 discuss this phenomenon and turn its disadvantage into an advantage, namely that of obtaining a
53 valid estimate of the oxygen isotopic composition of O_3 in the UT/LMS, an atmospheric
54 domain not yet covered by specific measurements. The air samples we examine in this study
55 were collected onboard a passenger aircraft carrying an airfreight container with analytical and
56 air/aerosol sampling equipment on long distance flights from Germany to South India and the
57 Caribbean within the framework of the CARIBIC project (Civil Aircraft for the Regular
58 Investigation of the atmosphere Based on an Instrument Container, [http://www.caribic-
59 atmospheric.com](http://www.caribic-atmospheric.com)).

60 2 Experimental and results

61 2.1 Whole air sampling

62 [4] CARIBIC-1 (Phase #1, abbreviated hereafter "C1") was operational from November 1998
63 until April 2002 using a Boeing 767-300 ER operated by LTU International Airlines
64 (Brenninkmeijer *et al.*, 1999). Using a whole air sample (WAS) collection system, twelve air
65 samples were collected per flight (of ~10 hours duration at cruise altitudes of 10–12 km) in
66 stainless steel tanks for subsequent laboratory analysis of the abundances of various trace gases,
67 including ^{14}CO . Large air samples were required in view of the ultra-low abundance of this
68 mainly cosmogenic tracer (10–100 molecules cm^{-3} STP, about 40–400 amol/mol). Each C1
69 WAS sample (holding ~350 litres of air STP) was collected within 15–20 min intervals
70 representing the integral of the compositions encountered along flight segments of ~250 km.
71 The overall uncertainty of the measured WAS [CO] is less than $\pm 1\%$ for the mixing ratio and
72 $\pm 0.1\%/\pm 0.2\%$ for $\delta^{13}C(CO)/\delta^{18}O(CO)$, respectively (Brenninkmeijer, 1993;
73 Brenninkmeijer *et al.*, 2001). Isotope compositions are reported throughout this manuscript
74 using $\delta^i = (R^i/R_{st}^i - 1)$ relating the ratio of rare over abundant isotopes R^i of interest (i denotes
75 ^{13}C , ^{18}O or ^{17}O) to the standard ratio R_{st}^i . These are V-SMOW of 2005.20×10^{-6} for $^{18}O/^{16}O$
76 (Gonfiantini, 1978; Coplen, 1994) and 386.72×10^{-6} for $^{17}O/^{16}O$ (Assonov and
77 Brenninkmeijer, 2003), and V-PDB of 11237.2×10^{-6} for $^{13}C/^{12}C$ (Craig, 1957), respectively. As
78 we mention above, the oxygen isotopic composition of the CO present in these WAS samples
79 was corrupted, in particular when O_3 levels were as high as 100–600 nmol/mol.

80 [5] CARIBIC-2 (Phase #2, referred to as "C2") started operation in December 2004 with a
Lufthansa Airbus A340-600 fitted with a new inlet system and air sampling lines, including

Deleted: ous effect

Deleted: the

Deleted: of receiving

Deleted: ozone

Deleted: . ¶
<#>Experimental¶
CARIBIC Phase #1
(abbreviated hereafter "C1")
was operational from
November 1998 until April
2002 using a Boeing 767-300
ER operated by LTU
International Airlines
(Brenninkmeijer *et al.*, 1999).
Here, twelve air samples were
collected per flight (of
~10 hours duration) in
stainless steel tanks for
analysing the abundance of
 ^{14}CO . For

Deleted: purpose, large

Deleted: are

Deleted: ozone

Deleted: , namely

Deleted: at cruise altitudes
of 10–12 km.

Deleted:

Deleted: (

81 PFA lined tubing for trace gas intake (Brenninkmeijer *et al.*, 2007). No flask CO mixing/isotope
82 ratio measurements are performed in C2.

2.2 On-line instrumentation

83 [6] In addition to the WAS collection systems, both C1 and C2 measurement setups include
84 different instrumentation for on-line detection of [CO] and [O₃] (hereinafter the squared
85 brackets [] denote the abundance, *i.e.* concentration or mixing ratio, of the respective species).
86 In situ CO analysis in C1 is done using a gas chromatography (GC)-reducing gas analyser
87 which provides measurements each 130 s with uncertainty of ±3 nmol/mol (Zahn *et al.*, 2000).
88 In C2, a vacuum ultraviolet fluorescence (VUV) instrument with lower measurement
89 uncertainty and higher temporal resolution of ±2 nmol/mol in ~2 s (Scharffe *et al.*, 2012) is
90 employed, respectively. Furthermore, the detection frequency for O₃ mixing ratios has also
91 increased, *viz.* from 0.06 Hz in C1 to 5 Hz in C2 (Zahn *et al.*, 2002; Zahn *et al.*, 2012).

2.3 Results

92 [7] When comparing the CO abundances in relation to O₃ mixing ratios for C1 and C2,
93 differences are apparent in the LMS, where C2 CO values are systematically lower. This is
94 illustrated in Figure 1 (a) which presents the LMS CO-O₃ distribution of the C2 measurements
95 overlaid with the C1 *in situ* and WAS data. For the *in situ* CO datasets we calculated the
96 statistics (*ibid.*, Panel (b)) of the samples with respective O₃ abundances clustered in
97 20 nmol/mol bins, *i.e.* the median and spread of [CO] as a function of [O₃] analysed. (The
98 [7]interquartile range, IQR, is used in the current analysis as a robust measure of the data
99 spread instead of the standard deviation.) The data exhibit large [CO] variations at [O₃] below
100 400 nmol/mol that primarily reflect pronounced seasonal variations in the NH tropospheric CO
101 abundance. With O₃ rising, [CO] increasingly becomes stratospheric, and its spread reduces to
102 mere 3.5 nmol/mol and less, as [O₃] surpasses 500 nmol/mol. Despite the comparable spread in
103 C1 and C2 [CO], from 400 nmol/mol of [O₃] onwards the C1 CO mixing ratios start to level off,
104 with no samples below 35 nmol/mol having been detected, whereas the C2 levels continuously
105 decline. By the 580 nmol/mol O₃ bin, C1 [CO] of 39.7^{+0.7}_{-1.3} nmol/mol accommodates some extra
106 15 nmol/mol compared to 25.6^{+1.2}_{-1.7} nmol/mol typical for C2 values. Overall, at [O₃] above
107 400 nmol/mol the conspicuously high [CO] is marked in about 200 *in situ* C1 samples, of which
108 158 and 69 emerge as statistically significant mild and extreme outliers, respectively, when
109 compared against the ample ($n \sim 3 \cdot 10^5$) C2 statistics. (The conventions here follow

Deleted: ..

Deleted: measurement is

Deleted: Nonetheless, when comparing the CO abundances in relation to O₃ mixing ratios for C1 and C2, differences are apparent in the LMS, where C2 CO values are systematically lower. Because the CO levels cannot have changed over the period in question by the difference we find (up to 55%), artefacts and calibration issues need to be scrutinised.

Deleted: whole air sample (

Deleted:)

Deleted: Thus, the in-

Deleted: C2

Deleted: versus ±3 nmol/mol each 130 s in C1 using a gas chromatography (GC)-reducing gas analyser (Zahn *et al.*, 2000;

Deleted: ..

Deleted:). In C2, no analyses of CO from whole air samples were made, in contrast to C1

Deleted: ozone

Deleted: ..

Deleted: ..

Deleted:

Deleted: C1 WAS samples for the laboratory analyses were collected in stainless steel tanks (holding ~350 litres of air STP) sampled within ~20 min intervals representing the integral of the compos[... [8]

Deleted:) of [CO] as a function of [O₃] analysed.

Deleted: (for C2, until June 2013)

Deleted: -

Deleted: (the

Deleted: of

Deleted: ‰.

110 Natrella (2003), *i.e.* ± 1.5 and ± 3 IQR ranges define the inner and outer statistical fences (ranges
111 outside which the data points are considered mild and extreme outliers) of the C2 [CO]
112 distribution in every O_3 bin, respectively; the statistics include the samples in bins with average
113 [O₃] of 420–620 nmol/mol. None of C1 CO at [O₃] above 560 nmol/mol agrees with the C2
114 observations. Because the CO levels cannot have changed over the period in question by the
115 difference we find (up to 55%), artefacts and calibration issues need to be scrutinised.

Deleted: ozone

Deleted: numbers quoted
are the sums for the C1 in-
situ CO falling

Deleted:).

116 [8] Unnatural elevations in the $^{18}O/^{16}O$ ratios of CO from WAS measurements are also evident,
117 as shown in Fig. 2. The large $\delta^{18}O(CO)$ departures that reach beyond +16‰ are found to be
118 proportional to the concomitant O_3 abundances (denoted with colour) and more prominent at
119 lower [CO] (see also Fig. S2 in the Supplementary Material). A rather different relationship,
120 however, is expected from our knowledge of UT/LMS CO sources (plus their isotope
121 signatures) and available *in situ* observations (*ibid.*, shown with triangles), as elucidated by
122 Brenninkmeijer *et al.* (1996) (hereafter denoted as “B96”). That is, the more stratospheric CO
123 is, the greater fraction of its local inventory is refilled with the photochemical component
124 stemming from methane oxidation with a characteristic $\delta^{18}O$ signature of $\sim 0\%$ or lower
125 (Brenninkmeijer and Röckmann, 1997). This occurs because the CO sink at ruling UT/LMS
126 temperatures proceeds more readily than its production, as the reaction of hydroxyl radical
127 (OH) with CO, being primarily pressure-dependent, outcompetes the temperature-sensitive
128 reaction of OH with CH₄. Furthermore, as the lifetime of CO quickly decreases with altitude,
129 transport-mixing effects take the lead in determining the vertical distributions of [CO] and
130 $\delta^{18}O(CO)$ above the tropopause, hence their mutual relationship. This is seen from the B96 data
131 at [CO] below 50 nmol/mol that line-up in a near linear relationship towards the end-members
132 with lowest $^{18}O/^{16}O$ ratios. These result from the largest share of the ^{18}O -depleted
133 photochemical component and extra depletion caused by the preferential removal of C¹⁸O in
134 reaction with OH (fractionation about $\sim 11\%$ at pressures below 300 hPa, Stevens *et al.*, 1980;
135 Röckmann *et al.*, 1998b).

Deleted: Besides the
mixing ratios, unnatural

Deleted: the

Deleted:).

Deleted: -

Deleted: ,

136 [9] It is beyond doubt that the enhancements of C1 $C^{18}O$ originate from O_3 , whose large
137 enrichment in heavy oxygen (above +60‰ in $\delta^{18}O$, Brenninkmeijer *et al.*, 2003) is typical and
138 found transferred to other atmospheric compounds (see Savarino and Morin (2012) for a
139 review). In Fig. 2 it is also notable that not only the LMS compositions are affected, but
140 elevations of (3–10)‰ from the bulk $\delta^{18}O(CO)$ values are present in more tropospheric samples
141 with [CO] of up to ~ 100 nmol/mol. These result from the dilution of the least affected
142 tropospheric air with high mixing ratios by CO-poor, however substantially contaminated,

Deleted: *i.e.*

Deleted: The latter equate
the

Deleted: CO sink

Deleted: ozone

Deleted: . (

Deleted:)

Deleted: unique

Deleted: , *i.e.*

143 stratospheric air, sampled into the same WAS tank. Such sampling-induced mixing renders an
144 unambiguous determination of the artefact source' isotope signature rather difficult, because
145 neither mixing nor isotope ratios of the admixed air portions are known sufficiently well (see
146 below).

147 [10] Differences between the WAS and *in situ* measured [CO] – a possible indication that the
148 $\delta^{18}\text{O}(\text{CO})$ contamination pertains specifically to the WAS data – average at $\bar{\Delta}_{\text{WAS}-\text{in situ}} =$
149 5.3 ± 0.2 nmol/mol (1 SD of the mean, $n = 408$) and happen to be random with respect to any
150 operational parameter or measured characteristic in C1, *i.e.* irrespective of CO or O₃
151 abundances. The quoted mixing ratio discrepancy remained after several calibrations between
152 the two systems had been performed, and likely results from the differences in the detection
153 methods, drifts of the calibration standards used (see details in Brenninkmeijer *et al.*, 2001) and
154 a short-term production of CO in the stainless steel tanks during sampling. The large spread of
155 $\Delta_{\text{WAS}-\text{in situ}}$ of ± 3.5 nmol/mol (1 σ of the population) ensues from the fact that the *in situ*
156 sampled air corresponds to (2–4)% of the concomitantly sampled WAS volume, as typically
157 6–7 *in situ* collections of ~5 s were made throughout one tank collection of 17–21 min. The
158 integrity of the WAS CO is further affirmed by the unsystematic distribution of the artefact
159 compositions among tanks (an opposite case for $\delta^{18}\text{O}(\text{CO}_2)$ in C1 is discussed by
160 Assonov *et al.*, 2009). Overall, the WAS and *in situ* measured CO mixing ratios correlate
161 extremely well (adj. $R^2 = 0.972$, slope of 0.992 ± 0.008 (1 σ), $n = 408$). However, both anomalies
162 in [CO] and $\delta^{18}\text{O}(\text{CO})$ manifest clear but complex functions of the concomitant [O₃]. That is,
163 the C1 *in situ* and WAS data very likely evidence artefacts pertaining to the O₃-driven effect of
164 the same nature. Below we ascertain and quantify these.

Deleted: -
Deleted:]
Deleted: data
Deleted: .

Deleted: . (
Deleted:)
Deleted: Δ_{WAS}
Deleted: .
Deleted: -
Deleted: -

Deleted: . (
Deleted:)
Deleted: -
Deleted: -
Deleted: ozone

165 3 Discussion

166 [11] Three factors may lead to the (artefact) distributions such as seen for C1 *in situ* [CO] at the
167 LMS O₃ abundances, namely:
168 [12] (i) Strong (linear) natural mixing, such as enhanced stratosphere-troposphere exchange
169 (STE), when a [CO] outside the statistically expected range results from the integration of air
170 having dissimilar ratios of the tracers' abundances, *viz.* $\rho_{\text{O}_3:\text{CO}} = [\text{O}_3]/[\text{CO}]$. For example, mixing
171 of two air parcels in a 15%:85% proportion (by moles of air) with typical $\rho_{\text{O}_3:\text{CO}}$ of 700:24
172 (stratospheric) and 60:125 (tropospheric), respectively, yields an integrated composition with
173 $\rho_{\text{O}_3:\text{CO}}$ of ~580:40 which indeed corresponds to C1 data (this case is exemplified by the mixing

Deleted: -
Deleted: ozone
Deleted: 1

174 curve in Fig. 1). Nonetheless, occurrences of rather high (compared to the typical
175 24–26 nmol/mol) stratospheric CO mixing ratios (in our case, ~40 nmol/mol at the concomitant
176 [O₃] of 500–600 nmol/mol) are rare. For instance, a deep STE similar to that described by
177 Pan *et al.* (2004) was observed by C2 only once (*cf.* the outliers at [O₃] of 500 nmol/mol in
178 Fig. 1), whereas the C1 outliers were exclusively registered in some 12 flights during
179 1997–2001. No relation between these outliers and the large-scale [CO] perturbation due to
180 extensive biomass burning in 1997/1998 (Novelli *et al.*, 2003) is established, otherwise elevated
181 CO mixing ratios should manifest themselves at lower [O₃] as well. Other tracers detected in
182 CARIBIC provide supporting evidence against such strongly STE-mixed air having been
183 captured by C1. That is, the binned distributions for the water vapour and de-trended N₂O
184 (similar to that for [CO] vs. [O₃] presented in Fig. 1, not shown here) are greatly similar in C1
185 and C2. Whereas the small relative variations in atmospheric [N₂O] merely confirm matching
186 [O₃] statistics in CARIBIC, the stratospheric [H₂O] distributions witness no $\rho_{O_3:H_2O}$ values
187 corresponding to the C1 outliers' $\rho_{O_3:CO}$, suggesting the latter being unnaturally low.

Deleted: ..

188 [13] (ii) Mixing effects can also occur artificially, originating from sampling peculiarities or data
189 processing. Since the CARIBIC platform is not stationary, about 5 s long sampling of an *in situ*
190 air probe in C1 implies integration of the compositions encountered along some hundred
191 metres, owing to the high aircraft speed. This distance may cover a transect between
192 tropospheric and stratospheric filaments of much different compositions. The effect of such
193 ‘translational mixing’ can be simulated by averaging the sampling data with higher temporal
194 frequency over longer time intervals. In this respect, the substantially more frequent CO data in
195 C2 (<1 s) were artificially averaged over a set of increasing intervals to reckon whether the long
196 sampling period in C1 could be the culprit for skewing its CO–O₃ distribution. As a result, the
197 original C2 data and their averages (equivalent to the C1 CO sample injection time) differ
198 negligibly, as do the respective $\rho_{O_3:CO}$ values; the actual C2 CO–O₃ statistic in the region of
199 interest ([O₃] of 540–620 nmol/mol) remains insensitive to integration of up to 300 s.
200 Furthermore, a very strong artificial mixing with an averaging interval of at least 1200 s
201 (comparable to C1 WAS sampling time) is required to yield the averages from the C2 data with
202 $\rho_{O_3:CO}$ characteristic for the C1 outliers.

Deleted: 2

Deleted: -

Deleted: C2

203 [14] (iii) In view of the above, it is unlikely that any natural or artificial mixing processes are
204 involved in the stratospheric [CO] discrepancies seen in C1. It therefore stands to reason to
205 conclude that the sample contamination in C1 occurred prior the probed air reaching the
206 analytical/sampling instrumentation in the container, since clearly elevated stratospheric CO

Deleted: 3

207 mixing ratios are common to WAS and *in situ* data. Two more indications, viz. growing [CO]
 208 discrepancy with increasing O₃ abundance, and the strong concomitant signal in δ¹⁸O(CO),
 209 imply that O₃-mediated photochemical production of CO took place. Further, by confronting the
 210 C1 and C2 [CO] measurements in a kinetic framework (detailed in Appendix A), we quantify
 211 the artefact CO component being chiefly a function of O₃ abundance as

$$C_c = b \cdot [O_3]^2, \quad b = (5.19 \pm 0.12) \cdot 10^{-5} \text{ [mol/nmol]}, \quad (1)$$

212 which is equivalent to 8–18 nmol/mol throughout the respective [O₃] range of
 213 400–620 nmol/mol (see Fig. 1 (d)). Subtracting this artefact signal yields the corrected *in situ*
 214 C1 CO–O₃ distribution conform to that of C2 (cf. red symbols in Fig. 1 (a)).

215 [15] Importantly, since we can quantify the contamination strength using only the O₃ abundance,
 216 the continuous *in situ* C1 [O₃] data allows to estimate the integral artefact CO component in
 217 each WAS sample and, if the isotope ratio of contaminating O₃ is known, to derive the initial
 218 δ¹⁸O(CO). The latter, as it was mentioned above, is subject to strong sample-mixing effects,
 219 which is witnessed by δ¹⁸O(CO) outliers even at relatively high [CO] up to 100 nmol/mol.
 220 Accounting for such cases is, however, problematic since it is necessary to distinguish the
 221 proportions of the least modified (tropospheric) and significantly affected (stratospheric)
 222 components in the resultant WAS sample mix. In reality, however, this information is not
 223 available, therefore we applied an *ad hoc* correction approach (which is capable of determining
 224 the contamination source (i.e., O₃) isotope signature as well), as described in the following.

3.1 Contamination isotope signatures

225 [16] Practically we resort to the differential mixing model (MM, originally known as the
 226 “Keeling-plot”), because it requires only the estimate of the artefact component mixing ratio,
 227 but no assumptions on the (unknown) shares and isotope signatures of the air portions mixed in
 228 a given WAS tank. The MM parameterises the admixing of the portion of artefact CO to the
 229 WAS sample with the “true” initial composition, as formulated below:

$$\begin{cases} {}^i\delta_a C_a = C_t {}^i\delta_t + C_c {}^i\delta_c \\ C_t \equiv (C_a - C_c) \end{cases}, \quad (2)$$

230 where indices *a*, *c* and *t* distinguish the abundances *C* and isotope compositions ^{*i*}δ (*i* may refer
 231 to ¹³C or ¹⁸O) pertaining to the analysed sample, estimated contamination and “true”
 232 composition sought (i.e., *C_t* and ^{*i*}δ_{*t*}), respectively. (Here the contamination strength *C_c* is derived

- Deleted: -
- Deleted: ozone
- Deleted: By
- Deleted: varying within
- Deleted: able
- Deleted: discover
- Deleted: signal being chiefly a function of O₃ abundance
- Deleted: . This allows using the in-situ
- Deleted: the
- Deleted: samples, specifically
- Deleted: s
- Deleted: and
- Deleted: . As
- Deleted: the WAS compositions are
- Deleted: which yield obvious
- Deleted: It is thus
- Deleted: and
- Deleted: ,
- Deleted: order to properly correct the composition of
- Deleted: On the other hand, the
- Deleted: should be
- Deleted: ozone
- Deleted: approach (MMA)
- Deleted: probe
- Deleted: A

233 | by integrating Eq. (1) using the *in situ* C1 [O₃] data for each WAS sample.) By rewriting the
234 | above equation w.r.t. the isotope signature of the admixed portion ${}^i\delta_c$, one obtains:

$${}^i\delta_c = {}^i\delta_i + ({}^i\delta_a - {}^i\delta_i)(1 + C_i/C_c), \quad (2)$$

235 | which signifies that linear regression of the measured ${}^i\delta_a$ as a function of the reciprocal of C_c
236 | yields the estimated contamination signature ${}^i\delta_c$ at $(C_c)^{-1} \rightarrow 0$. (The Keeling plot detailing the
237 | calculations with the MM is shown in Supplementary Material, Fig. S3.) The MM described by
238 | Eq. (2) provides adequate results only for the invariable initial compositions ($C_i, {}^i\delta_i$), therefore
239 | we apply it to the subsets of samples picked according to the same reckoned C_i (within a
240 | ± 2 nmol/mol window, $n > 7$). Such selection, however, may be insufficient: Due to the strong
241 | sampling effects in the WAS samples (see previous Section), it is possible to encounter samples
242 | that integrate different air masses to the same C_i but rather different average ${}^i\delta_i$. The solution in
243 | this case is to refer to the goodness of the MM regression fit, because the R^2 intrinsically
244 | measures the linearity of the regressed data, *i.e.* closeness of the “true” values in a regarded
245 | subset of samples, irrespective of underlying reasons for that.

246 | [17] Higher R^2 values thus imply higher consistency of the estimate, as demonstrated in Fig. 3
247 | showing the calculated ${}^i\delta_c$ for C_i below 80 nmol/mol as a function of the regression R^2 . The
248 | latter decreases with greater C_i (*i.e.*, larger sample subset size, since tropospheric air is more
249 | often encountered) and, conformably, larger variations in ${}^i\delta_i$. Ultimately, at lower R^2 the
250 | inferred ${}^{18}\text{O}$ signatures converge to values slightly above zero expected for uncorrelated data,
251 | *i.e.* C1 $\delta^{18}\text{O}(\text{CO})$ tropospheric average. A similar relationship is seen for the ${}^{13}\text{C}$ signatures
252 | (they converge around -28%), however, there are no consistent estimates found (R^2 is generally
253 | below 0.4). Since such is not the case for $\delta^{18}\text{O}$, the MM is not sufficiently sensitive to the
254 | changes caused by the contamination, which implies that the artefact CO $\delta^{13}\text{C}$ should be within
255 | the range of the “true” $\delta^{13}\text{C}(\text{CO})$ values. Interestingly, the MM is rather responsive to the
256 | growing fraction of the CH₄-derived component in CO with increasing [O₃], as the ${}^{13}\text{C}\delta_c$ value of
257 | $-(47.2 \pm 5.8)\%$ inferred at R^2 above 0.4 is characteristic for the $\delta^{13}\text{C}$ of methane in the UT/LMS.
258 | It is noteworthy that we have accounted for the biases in the analysed C1 WAS $\delta^{13}\text{C}(\text{CO})$
259 | expected from the mass-independent isotope composition of O₃ (see details in Appendix B).

260 | [18] We derive the “best-guess” estimate of the admixed CO ${}^{18}\text{O}$ signature at ${}^{18}\text{O}\delta_c =$
261 | $+(92.0 \pm 8.3)\%$, which agrees with the other MM results obtained at R^2 above 0.75. Taking the
262 | same subsets of samples, the concomitant ${}^{13}\text{C}$ signature matches ${}^{13}\text{C}\delta_c = -(23.3 \pm 8.6)\%$, indeed
263 | at the upper end of the expected LMS $\delta^{13}\text{C}(\text{CO})$ variations of $-(25-31)\%$, which likely does

Deleted: 1

Deleted: MMA

Deleted: 1

Deleted: A

Deleted: A

Deleted: A

Deleted: ozone

Deleted: estimates

264 | not allow the MM_v to ascertain this result as pertaining to the contamination (the corresponding
 265 | R^2 values are below 0.1). Upon the correction using the inferred ^{18}O δ_c value, the C1 WAS
 266 | $\delta^{18}\text{O}(\text{CO})$ data appear adequate (shown with red symbols in Fig. 2). That is, variations in the
 267 | observed C^{18}O are driven by (i) the seasonal/regional changes in the composition of
 268 | tropospheric air and by (ii) the degree of mixing or replacement of the latter with the
 269 | stratospheric component that is less variable in ^{18}O . This is seen as stretching of the scattered
 270 | tropospheric values ([CO] above 60 nmol/mol) in a mixing fashion towards $\delta^{18}\text{O}(\text{CO})$ of around
 271 | -10‰ at [CO] of ~ 25 nmol/mol, respectively. The corrected C1 $\delta^{13}\text{C}(\text{CO})$ data (shown in
 272 | Supplementary Material, Fig. S4) are found to be in a $\pm 1\text{‰}$ agreement with the observations by
 273 | B96, except for several deep stratospheric samples ([CO] below 40 nmol/mol). The latter were
 274 | encountered during "ozone hole" conditions and carried extremely low ^{13}C abundances, which
 275 | was attributed to the reaction of methane with available free Cl radicals
 276 | (Brenninkmeijer *et al.*, 1996).

3.2 Estimate of $\delta^{18}\text{O}(\text{O}_3)$

277 | [19] The ^{18}O δ_c signature inferred here (^{18}O $\delta_c = +92.0 \pm 8.3\text{‰}$) unambiguously pertains to O_3 and is
 278 | comparable to $\delta^{18}\text{O}(\text{O}_3)$ values measured in the stratosphere at temperatures about 30K lower
 279 | than those encountered in the UT/LMS by C1 (see Table 1 for comparison). If no other factors
 280 | are involved (see below), this discrepancy in $\delta^{18}\text{O}(\text{O}_3)$ should be attributed to the local
 281 | conditions, *i.e.* the higher pressures (typically 240–270 hPa for C1 cruising altitudes) at which
 282 | O_3 was formed. Indeed, the molecular lifetime (the period through which the species' isotope
 283 | reservoir becomes entirely renewed, as opposed to the "bulk" lifetime) of O_3 encountered along
 284 | the C1 flight routes is estimated on the order of minutes to hours at daylight (H. Riede, MPI-C,
 285 | 2010), thus the isotope composition of the photochemically regenerated O_3 resets quickly
 286 | according to the local conditions. Virtual absence of sinks, in turn, leads to "freezing" of the
 287 | $\delta^{18}\text{O}(\text{O}_3)$ value during night in the UT/LMS. Verifying the current $\delta^{18}\text{O}(\text{O}_3)$ estimate against the
 288 | kinetic data, in contrast to the stratospheric cases, is problematic. The laboratory studies on O_3
 289 | formation to date have scrutinised the concomitant kinetic isotope effects (KIEs) as a function
 290 | of temperature at only low pressures (50 Torr); the attenuation of the KIEs with increasing
 291 | pressure was studied only at room temperatures (see Table 1, also Brenninkmeijer *et al.* (2003)
 292 | for references). A rather crude attempt may be undertaken by conjecturing an inhibition of the
 293 | formation KIEs proportional to that measured at $\sim 320\text{K}$, however applied to the nominal low-
 294 | pressure values reckoned at (220–230)K. A decrease in $\delta^{18}\text{O}(\text{O}_3)$ of about (5.9–7.6)‰ is

Deleted: A

Deleted: 1

Deleted: 2

Deleted: substitution

Deleted: less variable in ^{18}O

Deleted: not

Deleted: here

Deleted: the

Deleted: 30

Deleted: in the

Deleted: ,

Deleted: <#>At last, the plausibility of the obtained results should be verified through the initial values singled out by the MMA, *i.e.* that the artefact CO was not admixed into the samples with unrealistic "true" compositions. The estimates presented here are based on $C_i = 69 \pm 1$ nmol/mol, ^{18}O $\delta_i = -(2.5 \pm 0.7)\text{‰}$ and ^{13}C $\delta_i = -(29.0 \pm 1.2)\text{‰}$ (1σ), which are compatible with the B96 observations as well.¶

Deleted: ozone

Deleted: the

Deleted: LMS

Deleted: ozone

Deleted: LMS case

Deleted: ozone

295 expected from such calculation, yet accounting for a mere one-half of the (13.3–14.6)%
296 "missing" in $^{18}\text{O}\delta_c$.

297 [20] Lower $^{18}\text{O}\delta_c$ values could result from possible isotope fractionation accompanying the
298 production of the artefact CO. Although not quantifiable here, oxygen KIEs in the $\text{O}_3 \rightarrow \text{CO}$
299 conversion chain cannot be ruled out, recalling that the intermediate reaction steps are not
300 identifiable and the artefact CO represents at most 4% of all O_3 molecules. Furthermore, the
301 yield λ_{O_3} of CO from O_3 may be lower than unity (see details in Appendix A). On the other
302 hand, the inference that the contamination strength primarily depends on $[\text{O}_3]$ indicates that the
303 kinetic fractionation may have greater effect on the carbon isotope ratios of the artefact CO
304 produced (the $^{13}\text{C}\delta_c$ values) in contrast to the oxygen ones. That is because all reactive oxygen
305 available from O_3 becomes converted to CO, whilst the concomitant carbon atoms are drawn
306 from a virtually unlimited pool whose apparent isotope composition is altered by the magnitude
307 of the ^{13}C KIEs.

308 [21] Besides KIEs, selectivity in the transfer of O atoms from O_3 to CO affects the resulting $^{18}\text{O}\delta_c$
309 value. The terminal O atoms in O_3 are enriched w.r.t. to the molecular (bulk) O_3 composition
310 when the latter is above $\sim+70\%$ in $\delta^{18}\text{O}$ (Janssen, 2005; Bhattacharya *et al.*, 2008), therefore an
311 incorporation of only central O atoms into the artefact CO molecules should result in a reduced
312 apparent $^{18}\text{O}\delta_c$ value. Such exclusive selection is, however, less likely from the kinetic
313 standpoint and was not observed in available laboratory studies (see Savarino *et al.* (2008) for a
314 review). For instance, Röckmann *et al.* (1998a) established the evidence of direct O transfer
315 from O_3 to the CO produced in alkene ozonolysis. A reanalysis of their results (in light of
316 findings of Bhattacharya *et al.* (2008)) suggests that usually the terminal atoms of the O_3
317 molecule become transferred (their ratio over the central ones changes from the bulk $\sim 2:1$ to
318 $\sim 1:0$ for various species). Considering the alternatives of the O transfer in our case (listed
319 additionally in Table 1), the equiprobable incorporation of the terminal and central O_3 atoms
320 into CO should result in the $\delta^{18}\text{O}(\text{O}_3)$ value in agreement with the "crude" estimate based on
321 laboratory data given above.

322 [22] Furthermore, the conditions that supported the reaction of O_3 (or its derivatives) followed by
323 the production of CO are vague. A few hypotheses ought to be scrutinised here. First, a fast
324 $\text{O}_3 \rightarrow \text{CO}$ conversion must have occurred, owing to short (*i.e.*, fraction of a second) exposure
325 time of the probed air to the contamination. Accounting for the typical C1 air sampling
326 conditions (these are: sampled air pressure of 240–270 hPa and temperature of 220–235K

Deleted: ozone

Deleted: artefact source

Deleted: corroborates

Deleted: all secondary O available from O_3 becomes converted to CO, *i.e.*

Deleted: effects here should be minimal. In this respect, the unknown ^{13}C KIEs

Deleted: play a more substantial (than

Deleted: ^{18}O KIEs) role in determining

Deleted: owing to the readily available C for

Deleted: artefact CO production. ¶ Besides KIEs,

Deleted: selectivity of the ozone

Deleted: may intervene

Deleted: expected to be

Deleted: ozone

Deleted: ,

Deleted: ,,

Deleted: lowering of the

Deleted: ozone

Deleted: atoms

Deleted: ozone

Deleted: ¶

Deleted: upheld

Deleted: ozone

Deleted: LMS

327 outboard to 275–300K inboard, sampling rate of $\sim 12.85 \cdot 10^{-3}$ moles s^{-1} corresponding to
328 350L STP sampled in 1200 s, inlet/tubing volume gauged to yield exposure times of 0.01 to
329 0.1 s due to variable air intake rate, $[O_3]$ of 600 nmol/mol), the overall reaction rate coefficient
330 (k_c in Eq. (A1) from Appendix A) must be on the order of $6 \cdot 10^{-15}/\tau_c$ [$\text{molec}^{-1} \text{cm}^3 \text{s}^{-1}$], where τ_c
331 is the exposure time. Assuming the case of a gas-phase CO production from a recombining O_3
332 derivative and an unknown carbonaceous compound X, the reaction rate coefficient for the
333 latter (k_r in Eq. (A1) in Appendix A) must be rather high, at least $\sim 6 \cdot 10^{-10}$ [$\text{molec}^{-1} \text{cm}^3 \text{s}^{-1}$]
334 over $\tau_c = 1/100$ s. This number decreases proportionally with growing τ_c and $[X]$, if we take less
335 strict exposure conditions. Nonetheless, in order to provide the amounts of artefact CO we
336 detect, a minimum abundance of 20 nmol/mol (or up to 4 μg of C per flight) of X is required,
337 which is not available in the UT/LMS from the species readily undergoing ozonolysis, e.g.
338 alkenes.

Deleted: ozone

339 [23] Second, a more complex heterogeneous chemistry on the inner surface of the inlet or
340 supplying tubing may be involved. Such can be the tracers' surface adsorption, (catalytic)
341 decomposition of O_3 and its reaction with organics or with surface carbon that also may lead to
342 the production of CO (Oyama, 2000). Evidence exists for the dissociative adsorption of O_3 on
343 the surfaces with subsequent production of the reactive atomic oxygen species (see, e.g.,
344 Li *et al.*, 1998, also Oyama, 2000). It is probable that sufficient amounts of organics have
345 remained on the walls of the sampling line exposed to highly polluted tropospheric air, to be
346 later broken down by the products of the heterogeneous decomposition of the ample
347 stratospheric O_3 . Unfortunately, the scope for a detailed quantification of intricate surface
348 effects in the C1 CO contamination problem is very limited.

Deleted: ozone

Deleted: ,

Deleted: . (

Deleted:)

Deleted: (

Deleted:)

Deleted: implex

349 4 Conclusions

350 [24] Recapitulating, the *in situ* measurements of CO and O_3 allowed us to unambiguously
351 quantify the artefact CO production from O_3 likely in the sample line of the CARIBIC-1
352 instrumentation. Strong evidence to that is provided by the isotope CO measurements. We
353 demonstrate the ability of the simple mixing model (“Keeling-plot” approach) to single out the
354 contamination isotope signatures even in the case of a large sampling-induced mixing of the air
355 with very different compositions. Obtained as a collateral result, the estimate of the $\delta^{18}O(O_3)$ in
356 the UT/LMS appears adequate, calling, however, for additional laboratory data (e.g., the

Deleted: -

Deleted: ozone

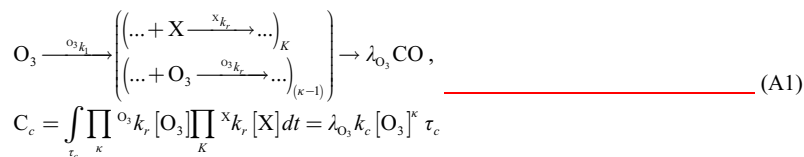
Deleted: (e.g., “Keeling-plot”

357 temperature-driven variations of the O₃ formation KIE at pressures above 100 hPa) for a more
 358 unambiguous verification.

359 Appendix A. Contamination kinetic framework

360 [25] We infer the O₃-exclusive functional dependence of the contamination strength C_c by
 361 discriminating the C1 outliers from respective C2 data in the following kinetic framework:

Deleted: ozone



362 where k_c denotes the overall pseudo-first-order rate coefficient of the reaction chain leading to
 363 the artefact CO production with the respective yield λ_{O₃}. The individual rate coefficients ^Xk_r and
 364 ^{O₃}k_r pertain to the unknown compound(s) X and O₃ reacting with the integral stoichiometry
 365 factors K and κ, respectively. Practically we find that variations in C_c are exhaustively described
 366 using [O₃], κ and k_c (the latter are obtained in a regression analysis). The value of k_c thus
 367 integrates the influence of the unknown (and likely invariable) [X], ^Xk_r and K. The relation
 368 defined by Eq. (A1) provides the best approximation for C_c as a function of [O₃] at κ =
 369 2.06±0.38, suggesting two chain steps involving O₃ or its derivatives. At κ = 2, the ratio
 370 C_c/[O₃]² (essentially proportional to the reaction time τ_c and overall rate coefficient k_c) is found
 371 to be (5.19±0.12)·10⁻⁵ mol/nmol (±1σ, adj. R² = 0.83, red. χ² = 4.0). The low uncertainty (within
 372 ±3%) of this estimate signifies an exclusive dependence of the contamination source on the O₃
 373 abundance, as well as much similar reaction times τ_c. It is possible to constrain the overall yield
 374 λ_{O₃} of CO molecules in the artefact source chain to be between 0.5 and 1, comparing the
 375 magnitude of C_c to the discrepancy between the [O₃] measured in C1 and C2 (±20 nmol/mol,
 376 taken equal to the [O₃] bin size owing to the N₂O–O₃ and H₂O–O₃ distributions matching well
 377 between the datasets). Lower λ_{O₃} values, otherwise, should have resulted in a noticeable (*i.e.*,
 378 greater than 20 nmol/mol) decrease in the C1 O₃ abundances with respect to the C2 levels.

Deleted: ozone

Deleted: (
 Deleted: /mol)⁻¹ (
 Deleted: a mere
 Deleted: ozone
 Deleted: comparable
 Deleted: C_s

379 **Appendix B. Corrections to measured $\delta^{13}\text{C}(\text{CO})$ values due to the oxygen**
 380 **MIF**

381 [26] Atmospheric O_3 carries an anomalous isotope composition (or mass-independent
 382 fractionation, MIF) with a substantially higher relative enrichment in ^{17}O over that in ^{18}O
 383 (above +25‰ in $\Delta^{17}\text{O} = (\delta^{17}\text{O}+1)/(\delta^{18}\text{O}+1)^\beta - 1$, $\beta = 0.528$) when compared to the majority of
 384 terrestrial oxygen reservoirs that are mass-dependently fractionated (*i.e.*, with $\Delta^{17}\text{O}$ of $\sim 0\text{‰}$)
 385 (see Brenninkmeijer *et al.* (2003) and refs. therein). CO itself also has an unusual oxygen
 386 isotopic composition, possessing a moderate tropospheric MIF of around +5‰ in $\Delta^{17}\text{O}(\text{CO})$
 387 induced by the sink KIEs in reaction of CO with OH (Röckmann *et al.*, 1998b;
 388 Röckmann *et al.*, 2002) and a minor source effect from the ozonolysis of alkenes
 389 (Röckmann *et al.*, 1998a; Gromov *et al.*, 2010). A substantial contamination of CO by O_3
 390 oxygen induces proportional changes to $\Delta^{17}\text{O}(\text{CO})$ that largely exceed its natural atmospheric
 391 variation. Furthermore, the MIF has implications in the analytical determination of $\delta^{13}\text{C}(\text{CO})$,
 392 because the presence of C^{17}O species interferes with the mass-spectrometric measurement of
 393 the abundances of ^{13}CO possessing the same basic molecular mass (m/e is 45). When inferring
 394 the exact $\text{C}^{17}\text{O}/\text{C}^{18}\text{O}$ ratio in the analysed sample is not possible, analytical techniques usually
 395 involve assumptions (*e.g.*, mass-dependently fractionated compositions or a certain non-zero
 396 $\Delta^{17}\text{O}$ value) with respect to the C^{17}O abundances (Assonov and Brenninkmeijer, 2001). In
 397 effect for the C1 CO data, the artefact CO produced from O_3 had contributed with unexpectedly
 398 high C^{17}O abundances that led to the overestimated $\delta^{13}\text{C}(\text{CO})$ analysed. Knowing the
 399 contamination magnitude C_c and assuming the typical O_3 MIF composition being $^{17}\text{O}\Delta_c$, the
 400 respective bias $^{13}\text{C}\delta_b$ is calculated using

$$\begin{cases} \Delta^{17}\text{O}(\text{CO}) \cong \left(^{17}\text{O}\Delta_t C_t + ^{17}\text{O}\Delta_c C_c \right) (C_a)^{-1} \\ ^{13}\text{C}\delta_b = 7.2568 \cdot 10^{-2} \Delta^{17}\text{O}(\text{CO}) \end{cases}, \quad (\text{B1})$$

401 where $^{17}\text{O}\Delta_t$ denotes the natural, *i.e.* expected “true” value of $\Delta^{17}\text{O}(\text{CO})$. The remaining
 402 parameters pertain to the contamination kinetic framework (see Appendix A, Eq. (A1)). For the
 403 purpose of the current estimate it is sufficient to take $^{17}\Delta_n$ of +5‰ representing equilibrium
 404 enrichments expected in the remote free troposphere and UT/LMS. For the O_3 MIF signature
 405 $^{17}\Delta_c$, the value of +30‰ (the average $\Delta^{17}\text{O}(\text{O}_3)$ expected from the kinetic laboratory data at
 406 conditions met along the C1 flight routes, see Sect. 3.2 and Table 1) is adopted. The coefficient
 407 that proportionates $^{13}\text{C}\delta_b$ and $\Delta^{17}\text{O}$ in Eq. (B1) is reckoned for the CO with initially unaccounted

Deleted: The $\delta^{13}\text{C}(\text{CO})$ values went through the ancillary correction owing to the specifics of the laboratory determination of the CO isotopologues' abundances by mass spectrometry.

Deleted: ..

Deleted: ..

Deleted: ..

Deleted: ..

Deleted: ozone

Deleted: ,

Deleted: ozone

408 MIF (e.g., the sample is assumed to be mass-dependently fractionated) and quantifies some
409 extra +0.73‰ in the analysed $\delta^{13}\text{C}(\text{CO})$ per every +10‰ of $\Delta^{17}\text{O}(\text{CO})$ excess (Assonov and
410 Brenninkmeijer, 2001). The most contaminated C1 WAS CO samples at $[\text{O}_3]$ above
411 300 nmol/mol are estimated to bear $\Delta^{17}\text{O}(\text{CO})$ of (6–12)‰ corresponding to fractions of
412 (0.10–0.27) of the artefact CO in the sample. Accordingly, the reckoned $\delta^{13}\text{C}(\text{CO})$ biases span
413 (0.5–0.9)‰. Although not large, these well exceed the $\delta^{13}\text{C}(\text{CO})$ measurement precision of
414 $\pm 0.1\%$ and were corrected for, and therefore are taken into account in the calculations with the
415 MM, presented in Sect. 3.1.

Deleted: ,

Deleted: probes

Deleted: A

416 Acknowledgements

417 [27] The authors are indebted to Claus Koeppel, Dieter Scharffe and Dr. Andreas Zahn for their
418 work and expertise on the carbon monoxide and ozone measurements in C1 and C2. Hella
419 Riede is acknowledged for comprehensive estimates of the species lifetimes along the
420 CARIBIC flight routes. We are grateful to Dr. Taku Umezawa, Dr. Angela K. Baker,
421 Dr. Emma C. Leedham and ACP reviewers for the helpful discussions and comments on the
422 manuscript.

Deleted: and

423 References

- 424 Assonov, S. S. and Brenninkmeijer, C. A. M.: A new method to determine the ^{17}O isotopic abundance in
425 CO_2 using oxygen isotope exchange with a solid oxide, *Rapid Commun. Mass Spectrom.*, **15**,
426 2426–2437, doi: [10.1002/rcm.529](https://doi.org/10.1002/rcm.529), 2001.
- 427 Assonov, S. S. and Brenninkmeijer, C. A. M.: A redetermination of absolute values for $^{17}\text{R}_{\text{VPDB-CO}_2}$ and
428 $^{17}\text{R}_{\text{VSMOW}}$, *Rapid Commun. Mass Spectrom.*, **17**, 1017–1029, doi: [10.1002/Rcm.1011](https://doi.org/10.1002/Rcm.1011), 2003.
- 429 Assonov, S. S., Brenninkmeijer, C. A. M., Koeppel, C., and Röckmann, T.: CO_2 isotope analyses using
430 large air samples collected on intercontinental flights by the CARIBIC Boeing 767, *Rapid Commun.*
431 *Mass Spectrom.*, **23**, 822–830, doi: [10.1002/rcm.3946](https://doi.org/10.1002/rcm.3946), 2009.
- 432 Bhattacharya, S. K., Pandey, A., and Savarino, J.: Determination of intramolecular isotope distribution of
433 ozone by oxidation reaction with silver metal, *J. Geophys. Res. Atm.*, **113**, D03303, doi:
434 [10.1029/2006jd008309](https://doi.org/10.1029/2006jd008309), 2008.
- 435 Brenninkmeijer, C. A. M.: Measurement of the abundance of ^{14}CO in the atmosphere and the $^{13}\text{C}/^{12}\text{C}$ and
436 $^{18}\text{O}/^{16}\text{O}$ ratio of atmospheric CO with applications in New Zealand and Antarctica, *J. Geophys. Res.*
437 *Atm.*, **98**, 10595–10614, doi: [10.1029/93JD00587](https://doi.org/10.1029/93JD00587), 1993.

438 Brenninkmeijer, C. A. M., Müller, R., Crutzen, P. J., Lowe, D. C., Manning, M. R., Sparks, R. J., and van
439 Velthoven, P. F. J.: A large ^{13}C O deficit in the lower Antarctic stratosphere due to “Ozone Hole”
440 Chemistry: Part I, Observations, *Geophys. Res. Lett.*, **23**, 2125–2128, doi: [10.1029/96gl01471](https://doi.org/10.1029/96gl01471), 1996.

441 Brenninkmeijer, C. A. M. and Röckmann, T.: Principal factors determining the $^{18}\text{O}/^{16}\text{O}$ ratio of
442 atmospheric CO as derived from observations in the southern hemispheric troposphere and lowermost
443 stratosphere, *J. Geophys. Res. Atm.*, **102**, 25477–25485, doi: [10.1029/97JD02291](https://doi.org/10.1029/97JD02291), 1997.

444 Brenninkmeijer, C. A. M., Crutzen, P. J., Fischer, H., Gusten, H., Hans, W., Heinrich, G.,
445 Heintzenberg, J., Hermann, M., Immelmann, T., Kersting, D., Maiss, M., Nolle, M., Pitscheider, A.,
446 Pohlkamp, H., Scharffe, D., Specht, K., and Wiedensohler, A.: CARIBIC – Civil aircraft for global
447 measurement of trace gases and aerosols in the tropopause region, *J. Atmos. Oceanic Technol.*, **16**,
448 1373–1383, doi: [10.1175/1520-0426\(1999\)016<1373:Ccafgm>2.0.Co;2](https://doi.org/10.1175/1520-0426(1999)016<1373:Ccafgm>2.0.Co;2), 1999.

449 Brenninkmeijer, C. A. M., Koepfel, C., Röckmann, T., Scharffe, D. S., Bräunlich, M., and Gros, V.:
450 Absolute measurement of the abundance of atmospheric carbon monoxide, *J. Geophys. Res. Atm.*, **106**,
451 10003–10010, doi: [10.1029/2000jd900342](https://doi.org/10.1029/2000jd900342), 2001.

452 Brenninkmeijer, C. A. M., Janssen, C., Kaiser, J., Röckmann, T., Rhee, T. S., and Assonov, S. S.: Isotope
453 effects in the chemistry of atmospheric trace compounds, *Chem. Rev.*, **103**, 5125–5161, doi:
454 [10.1021/Cr020644k](https://doi.org/10.1021/Cr020644k), 2003.

455 Brenninkmeijer, C. A. M., Crutzen, P., Boumard, F., Dauer, T., Dix, B., Ebinghaus, R., Filippi, D.,
456 Fischer, H., Franke, H., Frieß, U., Heintzenberg, J., Helleis, F., Hermann, M., Kock, H. H.,
457 Koepfel, C., Lelieveld, J., Leuener, M., Martinsson, B. G., Miemczyk, S., Moret, H. P.,
458 Nguyen, H. N., Nyfeler, P., Oram, D., O’Sullivan, D., Penkett, S., Platt, U., Pucek, M., Ramonet, M.,
459 Randa, B., Reichelt, M., Rhee, T. S., Rohwer, J., Rosenfeld, K., Scharffe, D., Schlager, H.,
460 Schumann, U., Slemr, F., Sprung, D., Stock, P., Thaler, R., Valentino, F., van Velthoven, P.,
461 Waibel, A., Wandel, A., Waschitschek, K., Wiedensohler, A., Xueref-Remy, I., Zahn, A.,
462 Zech, U., and Ziereis, H.: Civil Aircraft for the regular investigation of the atmosphere based on an
463 instrumented container: The new CARIBIC system, *Atmos. Chem. Phys.*, **7**, 4953–4976, doi:
464 [10.5194/acp-7-4953-2007](https://doi.org/10.5194/acp-7-4953-2007), 2007.

465 Coplen, T. B.: Reporting of stable hydrogen, carbon, and oxygen isotopic abundances (Technical Report),
466 *Pure Appl. Chem.*, **66**, 273–276, doi: [10.1351/pac199466020273](https://doi.org/10.1351/pac199466020273), 1994.

467 Craig, H.: Isotopic standards for carbon and oxygen and correction factors for mass-spectrometric analysis
468 of carbon dioxide, *Geochim. Cosmochim. Acta*, **12**, 133–149, doi: [10.1016/0016-7037\(57\)90024-8](https://doi.org/10.1016/0016-7037(57)90024-8),
469 1957.

470 Gonfiantini, R.: Standards for Stable Isotope Measurements in Natural Compounds, *Nature*, **271**, 534–536,
471 1978.

472 Gromov, S., Jöckel, P., Sander, R., and Brenninkmeijer, C. A. M.: A kinetic chemistry tagging technique
473 and its application to modelling the stable isotopic composition of atmospheric trace gases, *Geosci.*
474 *Model Dev.*, **3**, 337–364, doi: [10.5194/gmd-3-337-2010](https://doi.org/10.5194/gmd-3-337-2010), 2010.

475 Guenther, J., Erbacher, B., Krankowsky, D., and Mauersberger, K.: Pressure dependence of two relative
476 ozone formation rate coefficients, *Chem. Phys. Lett.*, **306**, 209–213, doi:
477 [10.1016/S0009-2614\(99\)00469-8](https://doi.org/10.1016/S0009-2614(99)00469-8), 1999.

478 Janssen, C., Guenther, J., Krankowsky, D., and Mauersberger, K.: Temperature dependence of ozone rate
479 coefficients and isotopologue fractionation in ^{16}O – ^{18}O oxygen mixtures, *Chem. Phys. Lett.*, **367**,
480 34–38, doi: [10.1016/S0009-2614\(02\)01665-2](https://doi.org/10.1016/S0009-2614(02)01665-2), 2003.

481 Janssen, C.: Intramolecular isotope distribution in heavy ozone ($^{16}\text{O}^{18}\text{O}^{16}\text{O}$ and $^{16}\text{O}^{16}\text{O}^{18}\text{O}$), *J. Geophys.*
482 *Res. Atm.*, **110**, D08308, doi: [10.1029/2004jd005479](https://doi.org/10.1029/2004jd005479), 2005.

483 Johnston, J. C. and Thiemeis, M. H.: The isotopic composition of tropospheric ozone in three
484 environments, *J. Geophys. Res. Atm.*, **102**, 25395–25404, doi: [10.1029/97jd02075](https://doi.org/10.1029/97jd02075), 1997.

485 Krankowsky, D., Bartecki, F., Klees, G. G., Mauersberger, K., Schellenbach, K., and Stehr, J.:
486 Measurement of heavy isotope enrichment in tropospheric ozone, *Geophys. Res. Lett.*, **22**, 1713–1716,
487 doi: [10.1029/95gl01436](https://doi.org/10.1029/95gl01436), 1995.

488 Krankowsky, D., Lämmerzahl, P., Mauersberger, K., Janssen, C., Tuzson, B., and Röckmann, T.:
489 Stratospheric ozone isotope fractionations derived from collected samples, *J. Geophys. Res. Atm.*, **112**,
490 D08301, doi: [10.1029/2006jd007855](https://doi.org/10.1029/2006jd007855), 2007.

491 Li, W., Gibbs, G. V., and Oyama, S. T.: Mechanism of Ozone Decomposition on a Manganese Oxide
492 Catalyst. 1. In Situ Raman Spectroscopy and Ab Initio Molecular Orbital Calculations, *J. Am. Chem.*
493 *Soc.*, **120**, 9041–9046, doi: [10.1021/ja981441+](https://doi.org/10.1021/ja981441+), 1998.

494 Mauersberger, K.: Measurement of Heavy Ozone in the Stratosphere, *Geophys. Res. Lett.*, **8**, 935–937,
495 doi: [10.1029/G1008i008p00935](https://doi.org/10.1029/G1008i008p00935), 1981.

496 Natrella, M.: NIST/SEMATECH e-Handbook of Statistical Methodsed., edited by: Croarkin, C. and
497 Tobias, P., NIST/SEMATECH, <http://www.itl.nist.gov/div898/handbook/> (last access: 07 May 2014),
498 2003.

499 Novelli, P. C., Masarie, K. A., and Lang, P. M.: Distributions and recent changes of carbon monoxide in
500 the lower troposphere, *J. Geophys. Res.*, **103**, 19015–19033, doi: [10.1029/98jd01366](https://doi.org/10.1029/98jd01366), 1998.

501 Novelli, P. C., Masarie, K. A., Lang, P. M., Hall, B. D., Myers, R. C., and Elkins, J. W.: Reanalysis of
502 tropospheric CO trends: Effects of the 1997–1998 wildfires, *J. Geophys. Res.*, **108**, 4464, doi:
503 [10.1029/2002jd003031](https://doi.org/10.1029/2002jd003031), 2003.

Deleted: /,

504 Oyama, S. T.: Chemical and Catalytic Properties of Ozone, *Catal. Rev. Sci. Eng.*, **42**, 279–322, doi:
505 [10.1081/cr-100100263](https://doi.org/10.1081/cr-100100263), 2000.

506 Pan, L. L., Randel, W. J., Gary, B. L., Mahoney, M. J., and Hints, E. J.: Definitions and sharpness of the
507 extratropical tropopause: A trace gas perspective, *J. Geophys. Res. Atm.*, **109**, D23103, doi:
508 [10.1029/2004jd004982](https://doi.org/10.1029/2004jd004982), 2004.

509 Röckmann, T., Brenninkmeijer, C. A. M., Neeb, P., and Crutzen, P. J.: Ozonolysis of nonmethane
510 hydrocarbons as a source of the observed mass independent oxygen isotope enrichment in tropospheric
511 CO, *J. Geophys. Res. Atm.*, **103**, 1463–1470, doi: [10.1029/97JD02929](https://doi.org/10.1029/97JD02929), 1998a.

512 Röckmann, T., Brenninkmeijer, C. A. M., Saueressig, G., Bergamaschi, P., Crowley, J. N.,
513 Fischer, H., and Crutzen, P. J.: Mass-independent oxygen isotope fractionation in atmospheric CO as a
514 result of the reaction CO+OH, *Science*, **281**, 544–546, doi: [10.1126/science.281.5376.544](https://doi.org/10.1126/science.281.5376.544), 1998b.

515 Röckmann, T., Jöckel, P., Gros, V., Bräunlich, M., Possnert, G., and Brenninkmeijer, C. A. M.: Using ¹⁴C,
516 ¹³C, ¹⁸O and ¹⁷O isotopic variations to provide insights into the high northern latitude surface CO
517 inventory, *Atmos. Chem. Phys.*, **2**, 147–159, doi: [10.5194/acp-2-147-2002](https://doi.org/10.5194/acp-2-147-2002), 2002.

518 Savarino, J., Bhattacharya, S. K., Morin, S., Baroni, M., and Doussin, J. F.: The NO+O₃ reaction: A triple
519 oxygen isotope perspective on the reaction dynamics and atmospheric implications for the transfer of
520 the ozone isotope anomaly, *J. Chem. Phys.*, **128**, 194303, doi: [10.1063/1.2917581](https://doi.org/10.1063/1.2917581), 2008.

521 [Savarino, J. and Morin, S.: The N, O, S Isotopes of Oxy-Anions in Ice Cores and Polar Environments, in:](#)
522 [Handbook of Environmental Isotope Geochemistry, edited by: Baskaran, M., Advances in Isotope](#)
523 [Geochemistry, Springer Berlin Heidelberg, 835–864, 2012.](#)

524 Scharffe, D., Slemr, F., Brenninkmeijer, C. A. M., and Zahn, A.: Carbon monoxide measurements onboard
525 the CARIBIC passenger aircraft using UV resonance fluorescence, *Atmos. Meas. Tech.*, **5**, 1753–1760,
526 doi: [10.5194/amt-5-1753-2012](https://doi.org/10.5194/amt-5-1753-2012), 2012.

527 Schinke, R., Grebenshchikov, S. Y., Ivanov, M. V., and Fleurat-Lessard, P.: Dynamical Studies Of The
528 Ozone Isotope Effect: A Status Report, *Annu. Rev. Phys. Chem.*, **57**, 625–661, doi:
529 [10.1146/annurev.physchem.57.032905.104542](https://doi.org/10.1146/annurev.physchem.57.032905.104542), 2006.

530 [Stevens, C. M., Kaplan, L., Gorse, R., Durkee, S., Compton, M., Cohen, S., and Bielling, K.: The Kinetic](#)
531 [Isotope Effect for Carbon and Oxygen in the Reaction CO+OH, *Int. J. Chem. Kinet.*, **12**, 935–948,](#) doi:
532 [10.1002/kin.550121205](https://doi.org/10.1002/kin.550121205), 1980.

533 Vicars, W. C., Bhattacharya, S. K., Erbland, J., and Savarino, J.: Measurement of the ¹⁷O-excess ($\Delta^{17}\text{O}$) of
534 tropospheric ozone using a nitrite-coated filter, *Rapid Commun. Mass Spectrom.*, **26**, 1219–1231, doi:
535 [10.1002/rcm.6218](https://doi.org/10.1002/rcm.6218), 2012.

536 Vicars, W. C. and Savarino, J.: Quantitative constraints on the ^{17}O -excess ($\Delta^{17}\text{O}$) signature of surface
537 ozone: Ambient measurements from 50°N to 50°S using the nitrite-coated filter technique, *Geochim.*
538 *Cosmochim. Acta*, **135**, 270–287, doi: [10.1016/j.gca.2014.03.023](https://doi.org/10.1016/j.gca.2014.03.023), 2014.

539 Zahn, A., Brenninkmeijer, C. A. M., Maiss, M., Scharffe, D. H., Crutzen, P. J., Hermann, M.,
540 Heintzenberg, J., Wiedensohler, A., Güsten, H., Heinrich, G., Fischer, H., Cuijpers, J. W. M., and van
541 Velthoven, P. F. J.: Identification of extratropical two-way troposphere-stratosphere mixing based on
542 CARIBIC measurements of O_3 , CO, and ultrafine particles, *J. Geophys. Res.*, **105**, 1527–1535, doi:
543 [10.1029/1999jd900759](https://doi.org/10.1029/1999jd900759), 2000.

544 Zahn, A., Brenninkmeijer, C. A. M., Asman, W. A. H., Crutzen, P. J., Heinrich, G., Fischer, H.,
545 Cuijpers, J. W. M., and van Velthoven, P. F. J.: Budgets of O_3 and CO in the upper troposphere:
546 CARIBIC passenger aircraft results 1997–2001, *J. Geophys. Res. Atm.*, **107**, 4337, doi:
547 [10.1029/2001jd001529](https://doi.org/10.1029/2001jd001529), 2002.

548 Zahn, A., Weppner, J., Widmann, H., Schlote-Holubek, K., Burger, B., Kühner, T., and Franke, H.: A fast
549 and precise chemiluminescence ozone detector for eddy flux and airborne application, *Atmos. Meas.*
550 *Tech.*, **5**, 363–375, doi: [10.5194/amt-5-363-2012](https://doi.org/10.5194/amt-5-363-2012), 2012.

552 Table 1. Ozone ¹⁸O/¹⁶O isotope ratios **from literature and this study**

Domain	T [K]	P [hPa]	$\delta^{18}\text{O}(\text{O}_3)$ [‰]	Remarks
Stratosphere	190–210	13–50	83–93 (<3)	¹
UT/LMS	220–235	240–270	89–95 (8)	²
			84–88 (6)	T
			91–98 (9)	TC
			112–124 (17)	C
Laboratory	190–210	~67	87–97 (6)	³
	220–235	~67	102–110 (6)	³
	220–235	240–270	95–103	⁴

Notes: Values in parentheses denote the average of the estimates' standard errors. The expected O_3 isotope composition on the V-SMOW scale is calculated from the O_3 enrichments ϵ reported relative to O_2 using $\delta^{18}\text{O}(\text{O}_3)_{\text{V-SMOW}} = \delta^{18}\text{O}(\text{O}_2)_{\text{V-SMOW}} + \epsilon^{18}\text{O}(\text{O}_3)_{\text{O}_2} + [\delta^{18}\text{O}(\text{O}_2)_{\text{V-SMOW}} \times \epsilon^{18}\text{O}(\text{O}_3)_{\text{O}_2}]$.

¹ Observations (see Krankowsky *et al.* (2007) and refs. therein), lowermost values (19–25 km). Quoted temperature range is derived by matching measured $\delta^{18}\text{O}(\text{O}_3)$ and laboratory data (see note ³).

² This study, C1 observations (10–12 km). Letters denote the estimates derived using the data from Bhattacharya *et al.* (2008) and assuming only terminal (T), only central (C) and equiprobable terminal and central (TC) O_3 atoms transfer to the artefact CO.

³ Calculated using the laboratory KIE temperature dependence data summarised by Janssen *et al.* (2003).

⁴ Calculated assuming a pressure dependence of the O_3 formation KIE similar to that measured at 320K (see Guenther *et al.* (1999) and refs. therein).

- Deleted: .
- Deleted: LMS
- Deleted: ^a
- Deleted: ^b
- Deleted: ^c
- Deleted: ^c
- Deleted: ^d
- Deleted: ozone
- Deleted: ozone
- Deleted: ^{a)}
- Deleted: ^c
- Deleted: ^{b)}
- Deleted: ozone
- Deleted: ^{c)}
- Deleted: ^{d)}

553 **Figure Captions**

554 Fig. 1. (a) Distribution of CO mixing ratios as a function of concomitant O_3 mixing ratios measured by
 555 CARIBIC in the LMS ($[O_3] > 300$ nmol/mol). The shaded area is the two-dimensional histogram of the C2
 556 measurements (all C2 data obtained until June 2013) counted in 5×1 nmol/mol size $[O_3] \times [CO]$ bins, thus
 557 darker areas emphasise greater numbers of particular CO– O_3 pairs observed. Small symbols denote the
 558 original C1 *in situ* measurements (black) and corrected for the artefacts (red); the C1 WAS analyses (11 of
 559 total 408) are shown with large symbols. Thin and thick step-lines demark the inner and outer statistical
 560 fences (ranges outside which the data points are considered mild or extreme outliers, see text) of the C2
 561 data, respectively. The dashed curve exemplifies compositions expected from the linear mixing of very
 562 different (e.g., tropospheric and stratospheric) end-members. (b) Statistics on CO mixing ratios from C1
 563 and C2 data shown in box-and-whisker diagrams for samples clustered in 20 nmol/mol O_3 bins (whiskers
 564 represent 9th/91st percentiles). (c) Sample statistic for each CARIBIC dataset (note the C2 figures scaled
 565 down by a factor of 1000). (d) Estimates of the C1 *in situ* CO contamination strength C_c as a function of
 566 $[O_3]$ (solid line) obtained by fitting the difference ΔCO between the C2 and C1 *in situ* $[CO]$ (small
 567 symbols) in the kinetic framework (see Appendix A, Eq. (A1)). Step line shows the ΔCO for the statistical
 568 averages (the shaded area equals the height of the inner statistical fences of the C2 data). Large symbols
 569 denote the estimates of C_c in the C1 WAS data (slight variations vs. the *in situ* data are due to the sample
 570 mixing effects, see Sect. 3). Colour denotes the respective C1 WAS $\delta^{18}O(CO)$ (note that typically 6–7
 571 *in situ* measurements correspond to one WAS sample). Note: The entire C1 CO/ O_3 dataset is presented in
 572 the Supplementary Material, Fig. S1.

Deleted: ozone

Deleted: -

Deleted: clustered in 20 nmol/mol O_3 bins

Deleted: ; box-and-whisker diagrams present the statistics for the C2 (black) and corrected C1 (red) data (whiskers represent 9th/91st percentiles).

Deleted: Lower panel presents the sample

573 Fig. 2. $^{18}O/^{16}O$ isotope composition of CO as a function of its reciprocal mixing ratio. Triangles present
 574 the data from the remote SH UT/LMS obtained by Brenninkmeijer *et al.* (1996) (B96). Colour refers to the
 575 concomitantly observed O_3 abundances; note the extremely low $[O_3]$ encountered by B96 in the Antarctic
 576 "ozone hole" conditions. Filled and hollow circles denote the original and corrected (as exemplified by the
 577 dashed arrow) C1 WAS data, respectively, with the symbol size scaling proportional to the estimated
 578 contamination magnitude (see text).

Deleted: -

579 Fig. 3. Results of the regression calculation with the MM. Shown with symbols are the contamination
 580 source isotope signatures δ_c as a function of the respective coefficient of determination (R^2). Colour
 581 denotes the number of samples in each subset selected. Solid and dashed lines present the best guess
 582 ± 1 SD for the $\delta^{18}O(O_3)$ and $\delta^{13}C(C_c)$ estimates. Dashed circles mark the values obtained at highest R^2 for
 583 $^{18}O\delta_i$ regression (above 0.9). See text for details.

Deleted: A.

Page 2: [1] Deleted	Sergey Gromov	19/10/2014 7:43 PM
<p>greater. It was soon realised that this phenomenon was due to the formation of CO in these tanks and/or in the sampling system and inlet tubing used, by reactions involving ozone (Brenninkmeijer et al., 1999).</p> <p>Unexpectedly high $^{18}\text{O}/^{16}\text{O}$ ratios in stratospheric ozone (O_3) were discovered by Konrad Mauersberger using a balloon-borne mass spectrometer (Mauersberger, 1981).</p>		
Page 2: [2] Deleted	Sergey Gromov	19/10/2014 7:43 PM
<p>the atypical ^{18}O and the subsequently discovered concomitant disproportionately high ^{17}O enrichments of stratospheric O_3 were subject to</p>		
Page 2: [3] Deleted	Sergey Gromov	19/10/2014 7:43 PM
<p>However, measurement of the</p>		
Page 2: [4] Deleted	Sergey Gromov	19/10/2014 7:43 PM
<p>ozone is generally problematic</p>		
Page 2: [5] Deleted	Sergey Gromov	19/10/2014 7:43 PM
<p>its concentrations may be higher</p>		
Page 2: [6] Deleted	Sergey Gromov	19/10/2014 7:43 PM
<p>helps a good deal to obtain information on the O_3 isotopic composition</p>		
Page 2: [7] Deleted	Sergey Gromov	19/10/2014 7:43 PM
<p>The air samples we refer to here were collected onboard a passenger aircraft carrying an airfreight container with analytical and air/aerosol sampling equipment on long distance passenger flights between Germany and South India/the Caribbean within the framework of the CARIBIC project (Civil Aircraft for the Regular Investigation of the atmosphere Based on an Instrument Container, http://www.caribic-atmospheric.com).</p>		
Page 4: [8] Deleted	Sergey Gromov	19/10/2014 7:43 PM
<p>C1 WAS samples for the laboratory analyses were collected in stainless steel tanks (holding ~350 litres of air STP) sampled within ~20 min intervals representing the integral of the compositions encountered along flight segments of ~250 km. The overall uncertainty of the measured WAS [CO] is less than $\pm 1\%$ for the mixing ratio and $\pm 0.1\%$/$\pm 0.2\%$ for $\delta^{13}\text{C}(\text{CO})/\delta^{18}\text{O}(\text{CO})$, respectively (Brenninkmeijer, 1993; Brenninkmeijer et al., 2001). The isotope compositions are reported throughout this manuscript using $\delta^i = ({}^iR/{}^iR_{\text{st}} - 1)$ relating the ratio of rare over abundant isotopes iR of interest (i denotes ^{13}C, ^{18}O or ^{17}O) to the standard ratio ${}^iR_{\text{st}}$. These are V-SMOW of 2005.20×10^{-6} for $^{18}\text{O}/^{16}\text{O}$ (Gonfiantini, 1978; Coplen, 1994) and 386.72×10^{-6} for $^{17}\text{O}/^{16}\text{O}$ (Assonov and Brenninkmeijer, 2003), and V-PDB of 11237.2×10^{-6} for $^{13}\text{C}/^{12}\text{C}$ (Craig, 1957), respectively.</p>		

New version of Fig. 1

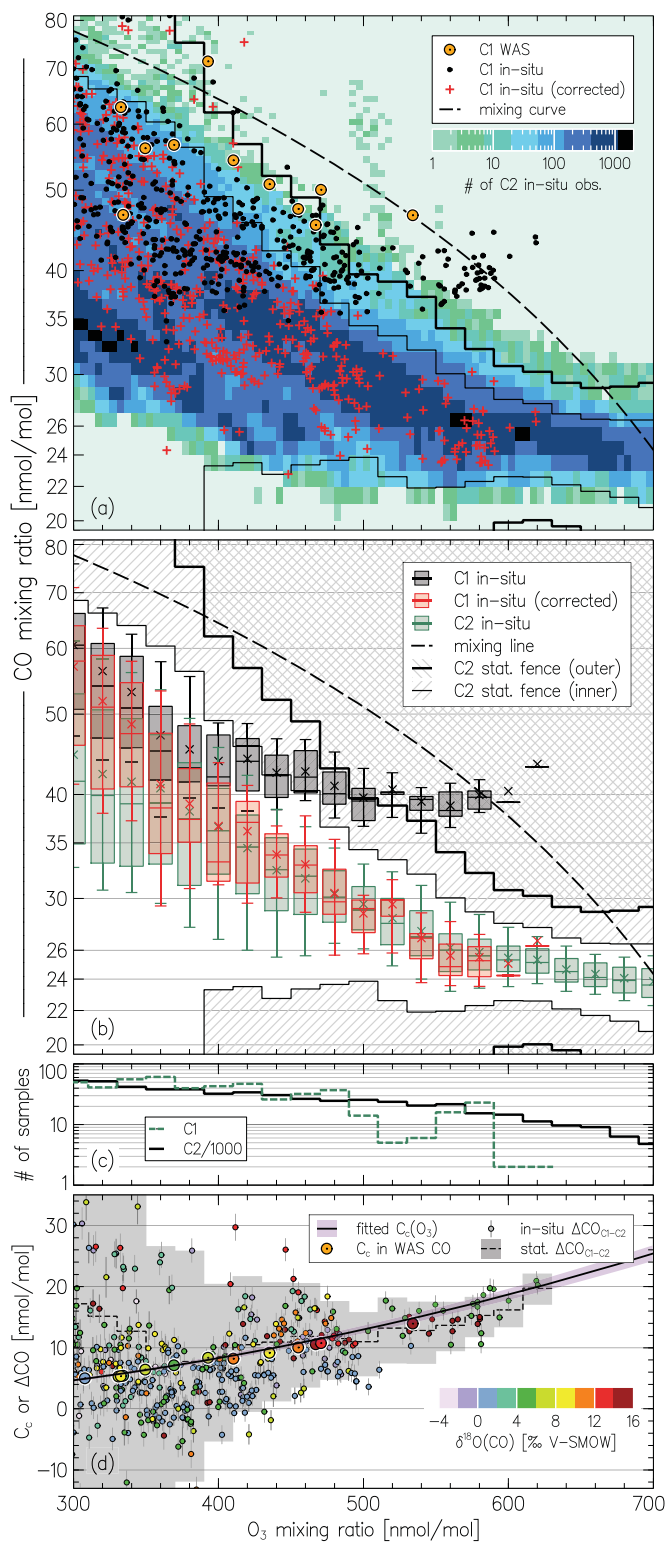


Fig. 1. (a) Distribution of CO mixing ratios as a function of concomitant O₃ mixing ratios measured by CARIBIC in the LMS ([O₃] > 300 nmol/mol). The shaded area is the two-dimensional histogram of the C2 measurements (all C2 data obtained until June 2013) counted in 5×1 nmol/mol size [O₃]×[CO] bins, thus darker areas emphasise greater numbers of particular CO–O₃ pairs observed. Small symbols denote the original C1 *in situ* measurements (black) and corrected for the artefacts (red); the C1 WAS analyses (11 of total 408) are shown with large symbols. Thin and thick step-lines demarcate the inner and outer statistical fences (ranges outside which the data points are considered mild or extreme outliers, see text) of the C2 data, respectively. The dashed curve exemplifies compositions expected from the linear mixing of very different (*e.g.*, tropospheric and stratospheric) end-members. (b) Statistics on CO mixing ratios from C1 and C2 data shown in box-and-whisker diagrams for samples clustered in 20 nmol/mol O₃ bins (whiskers represent 9th/91st percentiles). (c) Sample statistic for each CARIBIC dataset (note the C2 figures scaled down by a factor of 1000). (d) Estimates of the C1 *in situ* CO contamination strength C_c as a function of [O₃] (solid line) obtained by fitting the difference ΔCO between the C2 and C1 *in situ* [CO] (small symbols) in the kinetic framework (see Appendix A, Eq. (A1)). Step line shows the ΔCO for the statistical averages (the shaded area equals the height of the inner statistical fences of the C2 data). Large symbols denote the estimates of C_c in the C1 WAS data (slight variations *vs.* the *in situ* data are due to the sample mixing effects, see Sect. 3). Colour denotes the respective C1 WAS $\delta^{18}\text{O}(\text{CO})$ (note that typically 6–7 *in situ* measurements correspond to one WAS sample). Note: The entire C1 CO/O₃ dataset is presented in the Supplementary Material, Fig. S1.

Updated Fig. 2

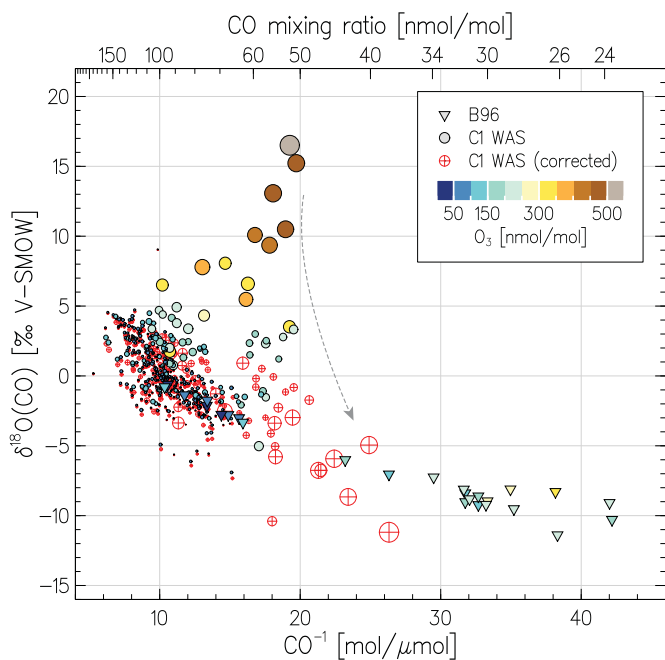


Fig. 2. $^{18}\text{O}/^{16}\text{O}$ isotope composition of CO as a function of its reciprocal mixing ratio. Triangles present the data from the remote SH UT/LMS obtained by Brenninkmeijer *et al.* (1996) (B96). Colour refers to the concomitantly observed O_3 abundances; note the extremely low $[\text{O}_3]$ encountered by B96 in the Antarctic "ozone hole" conditions. Filled and hollow circles denote the original and corrected (as exemplified by the dashed arrow) C1 WAS data, respectively, with the symbol size scaling proportional to the estimated contamination magnitude (see text).